Progress In Electromagnetics Research M, Vol. 69, 185–195, 2018

Dual-Band Dual-Sense Circularly Polarized Asymmetric Slot Antenna with F-Shaped Feed Line and Parasitic Elements

Rohit K. Saini* **and Pritam S. Bakariya**

Abstract—A novel dual-band and dual-sense circularly polarized coplanar waveguide (CPW) fed planar antenna with an asymmetric rectangular slot is presented. An F-shaped feed line is protruded from the signal line into the slot. Circular polarization is obtained due to the F-shaped feed line and asymmetry in the slot. Axial ratio bandwidth is significantly enhanced by placing parasitic elements adjacent to the feedline. The antenna has a size of $63.5 \times 55\ \text{mm}^2$. The measured results agree well with simulation. The measured impedance bandwidths are 26.04% (1.57 GHz–2.04 GHz) for the lower band and 18.93% (2.87 GHz–3.47 GHz) for the upper band. The measured 3 dB axial ratio bandwidths of lower band and upper bands are 22.22% (1.6 GHz–2 GHz) and 10.53% (3.15 GHz–3.5 GHz), with respect to 1.8 GHz (RHCP) and 3.325 GHz (LHCP), respectively.

1. INTRODUCTION

In recent years, the demand for high speed data transfer and multifunction capability in wireless devices has increased significantly. Therefore, dual-band dual-sense and broadband circularly polarized planar antenna has attracted high attention of antenna researchers. Printed circularly polarized (CP) antennas have become the most promising candidate to fulfill the demand of modern wireless communication system which includes small size and light weight for portable device and most important its ability to combating with multipath fading effect. Due to its special feature of circularly polarization, CP antennas are insensitive to alignments and orientation of transmitting or receiving antennas which reduce the effect of multipath fading, make the CP antenna eligible and highly efficient to be used in wireless communication application including the satellites communication and broadcasting.

Coplanar waveguide (CPW) fed wideband circularly polarized slot antennas have drawn more attraction over microstrip feed due to their various advantages such as low radiation loss, low dispersion, and scope of easy integration with solid state devices [1–7]. A dual-band circularly polarized slot antenna is proposed in [8]. However, this antenna has the same sense of polarization in both the bands. Dual-band, dual-sense circular polarization is beneficial to minimization of interference effect. The antenna presented in [9] uses two spiral slots loaded at the left corners of the ground plane for dual-band dual-sense operation. A dual-band, dual-sense CP antenna fed by microstrip line is designed in [10], and those fed by CPW are presented in [11–13]. Two-port antenna configurations for wideband dual-sense [14, 15] and dual-band, dual-sense [16] for polarization diversity systems are presented.

In this paper, a CPW-fed slot antenna with an asymmetric rectangular slot, F-shaped feed line and parasitic elements is designed for dual-band and dual-sense circular polarization. The proposed antenna can generate right- and left-hand circularly polarizations (RHCP and LHCP) in lower and upper bands in $+z$ directions, respectively. The proposed CP slot antenna has low profile, compact size and simple structure which make it suitable for wireless communication, radar and satellite communication.

Received 2 April 2018, Accepted 13 May 2018, Scheduled 19 June 2018

* Corresponding author: Rohit Kumar Saini (rohitccsu@gmail.com).

The authors are with the Department of Electronics and Communication Engineering, S R Engineering College, Warangal 506371, India.

The organization of this paper is as follows. The proposed antenna structure with design principle is introduced in Section 2. Section 3 describes the CP mechanism with the help of magnetic current distribution. Section 4 outlines the antenna parametric study. In Section 5, the measured results of prototype are discussed and compared with simulation. The conclusions are given in Section 6.

2. ANTENNA CONFIGURATION

The CPW-fed slot antenna with an asymmetric rectangular slot and F-shaped feed line is shown in Figure 1. The F-shape feed line and asymmetry in the slot result in dual-band and dual-sense circular polarization. Rectangle shape parasitic elements (PE1 and PE2) and strip are used to enhance axial ratio bandwidth. The antenna has a compact size of $63.5 \times 55\,\text{mm}^2$. This antenna is printed on an FR4 substrate of 1.6 mm thickness with a dielectric constant of 4.4 and loss tangent of 0.02. The antenna is fed by a $50\,\Omega$ CPW feed having signal line of width 3.2 mm and two identical gaps of 0.7 mm with ground plane. The F-shaped feed line is protruded from the signal line into the slot. The horizontal (length L_{s2}) and vertical (length Ls_3) line sections of the F-shaped feed line are separated from ground plane with gaps of 1.2 mm and 1.75 mm, respectively.

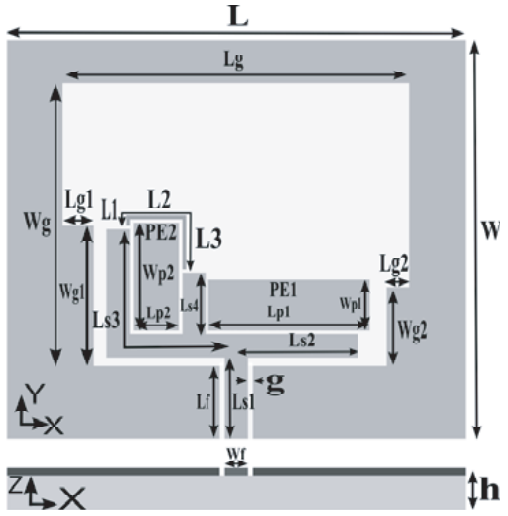

Figure 1. Geometry of the proposed CPW-fed antenna. ($L = 63.5$, $W = 55$, $L_g = 48.1$, $W_g = 39.2$, $L_{g1} = 4.3$, $W_{g1} = 19.4$, $L_{g2} = 3.1$, $W_{g2} = 10.9$, $W_f = 3.2$, $L_f = 10$, $g = 0.7$, $h = 1.6$, $L_{s1} = 11.2$, $L_{s2} = 16.8$, $L_{s3} = 32.5$, $L_{s4} = 8.4$, $L_{p1} = 22.5$, $W_{p1} = 7$, $L_{p2} = 6.2$, $W_{p2} = 15$, $L_1 = 1$, $L_2 = 8.2$, and $L_3 = 7$) (Unit: millimeters).

The rectangle-shaped parasitic elements (PE1 and PE2) have dimensions of $22.5 \times 7\,\text{mm}^2$ and $15 \times 6.2\,\text{mm}^2$, respectively. The strip line of length 16.2 mm and width 0.5 mm is separated from parasitic element (PE2) with a gap of 0.5 mm. Parasitic elements (PE1 and PE2) are also separated from the F-shaped signal line with a gap of 0.5 mm from both sides. In addition to the CPW feed and F-shaped signal line, asymmetry is introduced in the slot at the left and right lower corners as shown in Figure 1.

3. CIRCULAR POLARIZATION MECHANISM

Magnetic current distributions in the slot of the proposed antenna at center frequency 1.75 GHz of lower band at two time instants: $\omega t = 0°$, $90°$ viewed from the $+Z$ direction are shown in Figure 2(a) to perceive why the circular polarization can be generated by the designed antenna. As the magnetic current rotates anticlockwise with increase of time phase, the fields radiated will be RHCP in $+Z$ direction and LHCP in the $-Z$ direction.

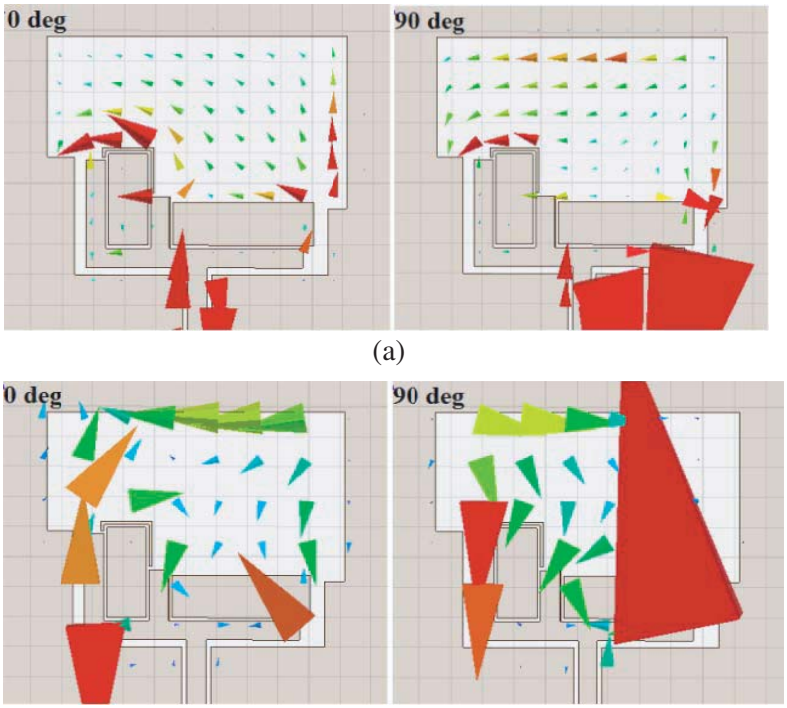

Figure 2. Magnetic current distribution at (a) 1.75 GHz and (b) 3.3 GHz for proposed antenna at two different time instants: $\omega t = 0°$ and 90°.

Magnetic current distributions in the slot of the proposed antenna at center frequency 3.3 GHz of upper band at two time instants: $\omega t = 0°$, 90° viewed from the $+Z$ direction areshown in Figure 2(b). As the magnetic current rotates clockwise with increase of time phase, the fields radiated will be LHCP in $+Z$ direction and RHCP in the $-Z$ direction. It can be shown that the magnetic current distributions at $\omega t = 180°$ and 270° are equal in magnitude and opposite in phase of $\omega t = 0°$ and 90° in both the cases.

4. ANTENNA DESIGN

At first, steps of improvement of the proposed antenna are described by four prototypes (Figure 3): Ant. 1 includes only an F-shaped feed line; Ant. 2 contains an F-shaped feed line and a rectangle-shaped parasitic element (PE1); Ant. 3 has an F-shaped feed line and two rectangular shaped parasitic elements (PE1 and PE2). Ant. 4 has an F-shaped feed line, two rectangle-shaped parasitic elements (PE1 and PE2) and a strip.

The F-shape feed is protruded from the signal line into the slot. The rectangular slot of length L_g and width W_g behaves as a lossy resonator. Loss is mainly due to radiation. Feed line has three branches. By a proper choice of L_{s2} and L_{s3}, two orthogonal components of magnetic current of same magnitude and quadrature phase can be generated inside the rectangular slot. If the slot is excited by the right side branch of length L_{s2}, magnetic current rotates anticlockwise which results in RHCP in positive z direction. For this case, left side branch acts as an open-stub which helps in impedance matching. Similarly, LHCP can be excited by using the left side branch of length L_{s3}. For the RHCP, $L_{s2}+L_{s1}$ is approximately odd multiple of $\lambda_g/4$, where λ_g is the guided wavelength at the mid-band frequency. $\lambda_g = \lambda_o/\sqrt{\varepsilon_e}$, where λ_0 is the free space wavelength and $\varepsilon_e = (\varepsilon_r + 1)/2$. Similarly, $L_{s3}+L_{s1}$ should be approximately odd multiple of $\lambda_g/4$ at the mid-band frequency for the LHCP. Depending on the application requirements, a lower operating frequency for the RHCP or LHCP can be selected. Diagonal length of the slot is taken approximately half of the guided wavelength at the mid-band frequency of the lower band. All the dimensions are kept to the optimized values.

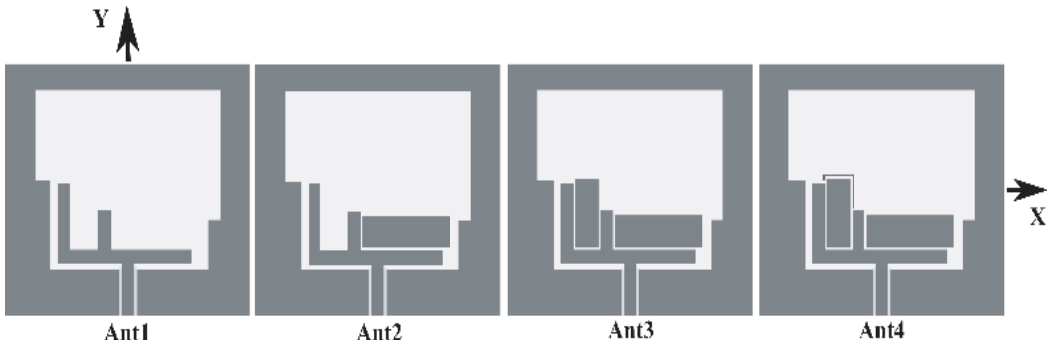

Figure 3. Four improved prototypes of the proposed antenna.

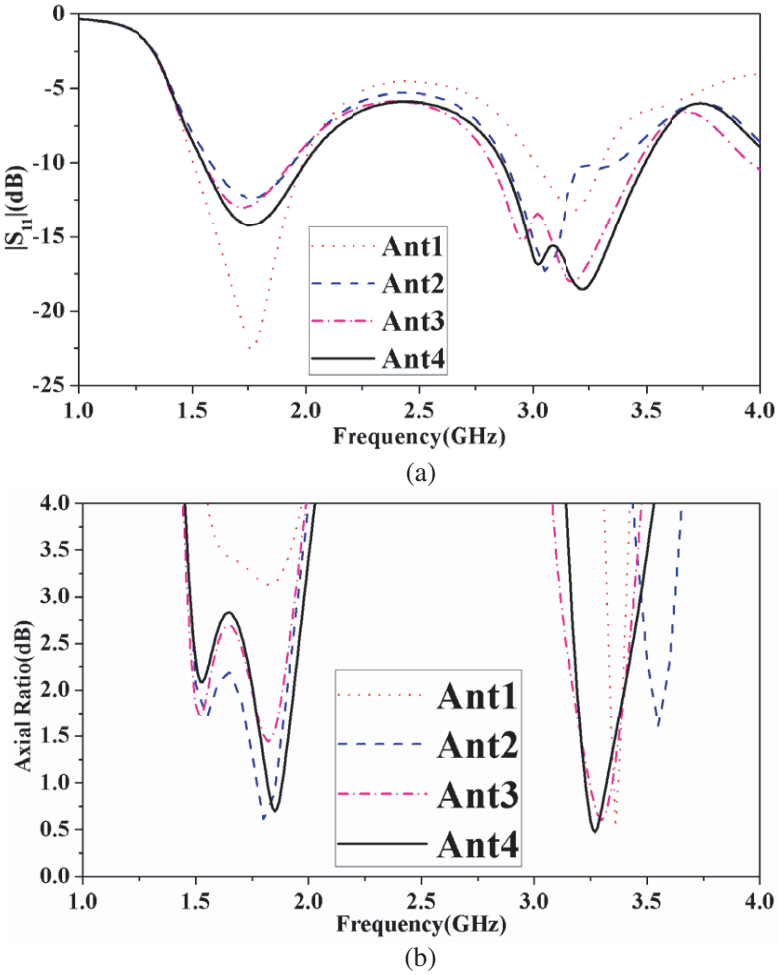

Figure 4. Simulated S_{11} and AR for antennas 1–4 (for antennas with optimized values of the design parameters summarized in Figure 1).

The simulated results for four antennas are plotted in Figure 4. It shows that only F-shaped feed line can generate circular polarization. However, since the feed dimension must be adjusted individually for the RHCP and LHCP excitations, the same antenna cannot be used for two bands having opposite senses of polarization. However, it is observed that dual-band and dual-sense CP can be obtained using two additional rectangular parasitic elements inside the rectangular slot. Improvement steps

using parasitic elements are described by two prototypes Ant. 2 and Ant. 3 as shown also in Figure 3. Then, by placing rectangular shaped parasitic element (PE1), wide bandwidth circular polarization was generated in the lower band. However, in upper band, bandwidth is still narrow, and impedance mismatch is there during circular polarization. By adding another rectangular shaped parasitic element (PE2) along with PE1, circular polarization bandwidth of upper band was increased significantly, and impedance matching was obtained. Addition of a strip adjacent to PE1 increases axial ratio bandwidth of lower band by about 1.3%.

5. NUMERICAL ANALYSIS AND PARAMETRIC STUD

In order to achieve the best performance for dual-band, dual-sense circular polarization, a series of parametric variations has been done. By optimizing different parameters one by one to find their effect on the impedance and axial ratio bandwidth of the antenna, the optimized size of the antenna has been selected. Parametric studies have been carried out by the HFSS simulator. Throughout the studies presented in this section, all other parameters that have not been mentioned are fixed to the values shown in Figure 1.

5.1. Step One: The Effect of Parasitic Element (PE1) Size

Figures 5(a) and (b) show the effect of variation in sizes of PE1 on impedance and axial ratio bandwidth. It is observed that increase of size of parasitic element PE1 increases the axial ratio bandwidths of both bands. Based on an overall consideration, the size of PE1 is selected as $7 \times 22.5\,\text{mm}^2$.

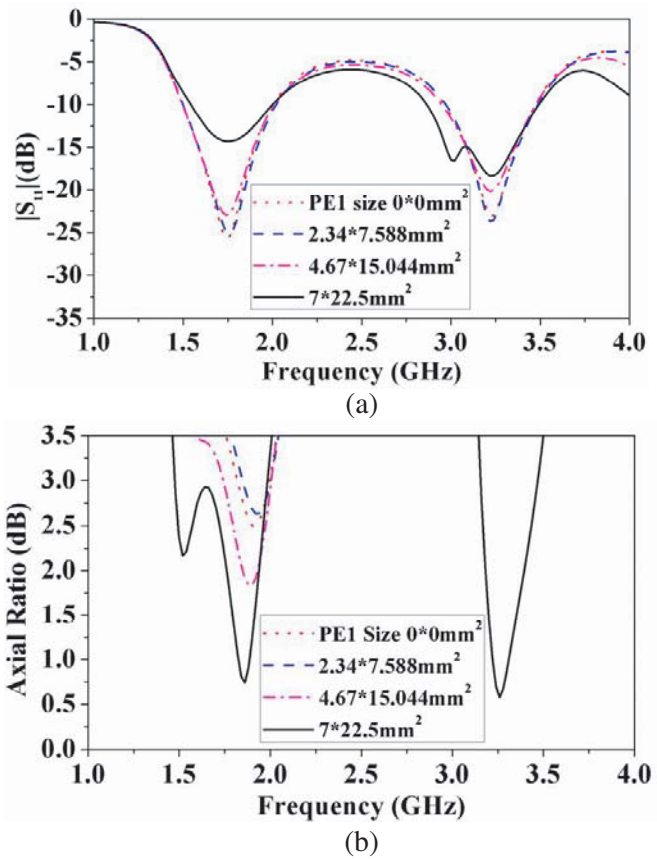

Figure 5. Effect of the size of PE1on antenna parameters: (a) S_{11} (dB); (b) Axial ratio (dB) (in $+z$ direction).

5.2. Step Two: The Effect of Parasitic Element (PE2) Size

Figures 6(a) and (b) show the effect of the size of PE2 on the impedance and axial ratio bandwidth. It shows that impedance matching and axial ratio bandwidth got best results when the size of the PE2 was $6.2 \times 15\,\text{mm}^2$.

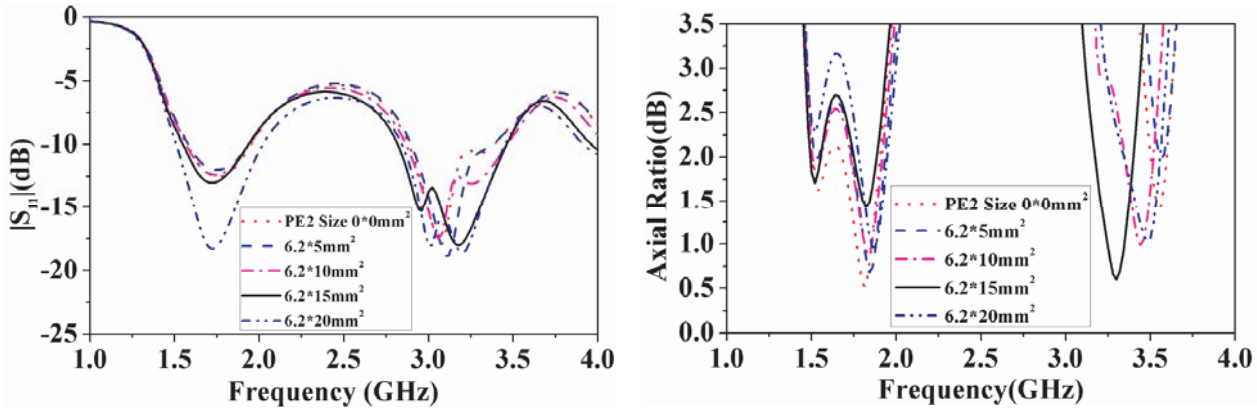

(a) (b)

Figure 6. Effect of the size of PE2 on antenna parameters: (a) S_{11} (dB); (b) Axial ratio (dB) (in $+z$ direction).

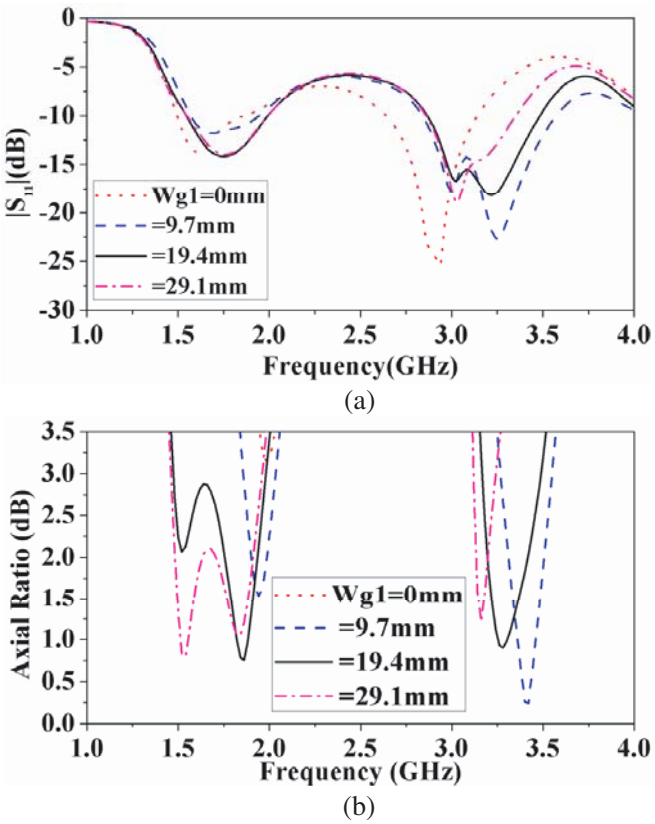

(a)

(b)

Figure 7. Effect of the slot perimeter (W_{g1}) on antenna parameters: (a) S_{11} (dB); (b) Axial ratio (in $+z$ direction).

5.3. Step Three: The Effect of Asymmetric Slot Parameters W_{g1} and W_{g2}

Figures 7 and 8 show the effect of asymmetric slot parameters W_{g1} and W_{g2} of the ground plane of the slot antenna. Introduction of the asymmetry in the ground plane significantly improves the axial ratio bandwidth in the lower band. When $W_{g1} = 0$ mm, no circular polarization was obtained in both the bands. With increase of W_{g1}, upper band was shifted towards lower frequency. It is observed that both impedance matching and axial ratio bandwidth in both the bands would be best when $W_{g1} = 19.4$ mm and $W_{g2} = 10.9$ mm.

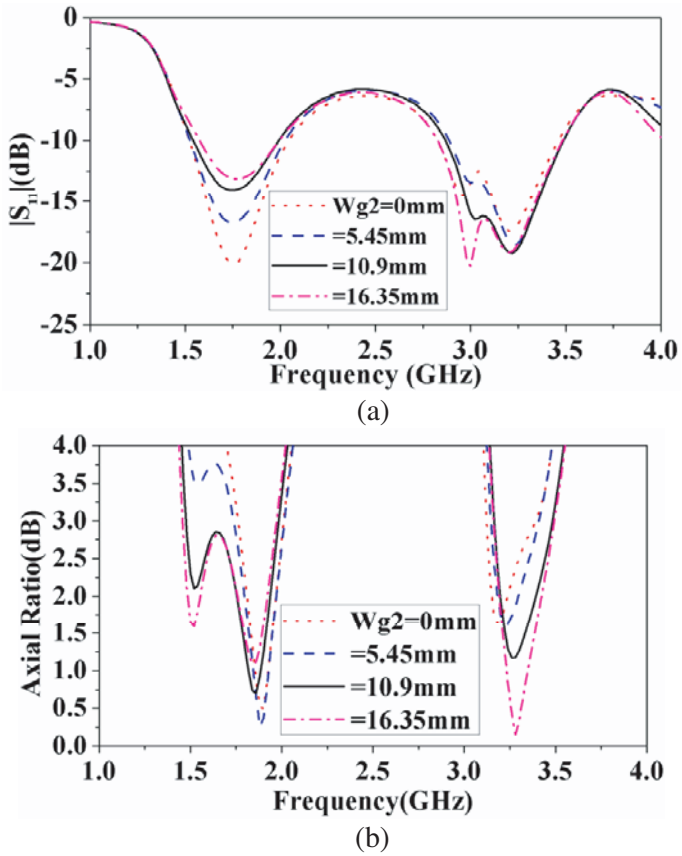

Figure 8. Effect of the slot perimeter (W_{g2}) on antenna parameters: (a) S_{11} (dB); (b) Axial ratio (in $+z$ direction).

6. SIMULATION AND MEASUREMENT RESULTS

According to the results of simulation, the optimized dimensions of the proposed antenna are shown in Figure 1. Figure 9 shows a photograph of the fabricated antenna. The measured results of the impedance bandwidth ($S_{11} \leq -10$ dB) are about 470 MHz from 1.57 GHz to 2.04 GHz, which is 26.04% with respect to the central frequency 1.805 GHz for lower band (RHCP) and 600 MHz from 2.87 GHz to 3.47 GHz, which is 18.93% with respect to 3.17 GHz for upper band (LHCP) as shown in Figure 10. The measured 3-dB axial ratio bandwidth is 400 MHz from 1.6 GHz to 2 GHz, which is 22.22% with respect to the central frequency 1.8 GHz for lower band (RHCP) and 350 MHz from 3.15 GHz to 3.5 GHz, which is 10.53% with respect to central frequency 3.325 GHz for upper band (LHCP) as shown in Figure 11.

Figure 12 shows the simulated and measured gains against frequency, which vary from 2.5 dB to 3.6 dB and 0.5 dB to 1.5 dB in lower and upper bands. The simulated and measured antenna efficiencies are shown in Figure 13. The measured antenna efficiency is more than 90% in both the bands. Figure 14 shows the measured normalized RHCP and LHCP radiation patterns at 1.8 GHz and 3.3 GHz. At

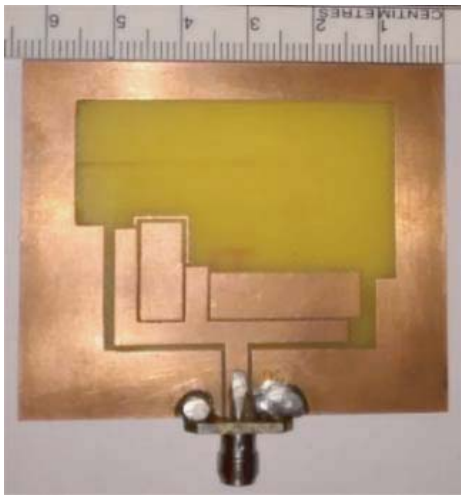

Figure 9. Photograph of fabricated antenna.

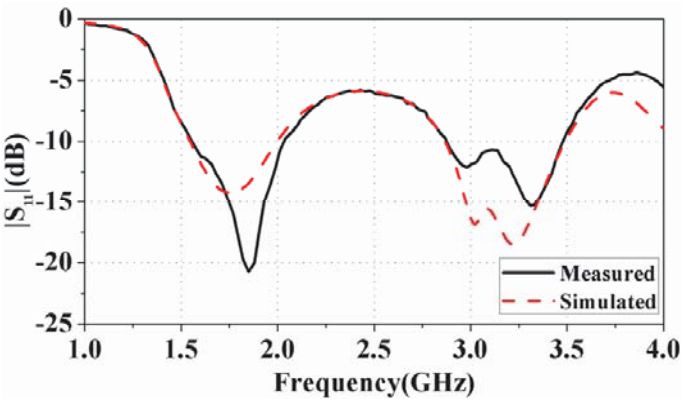

Figure 10. Measured and simulated S_{11} (dB) of the proposed antenna.

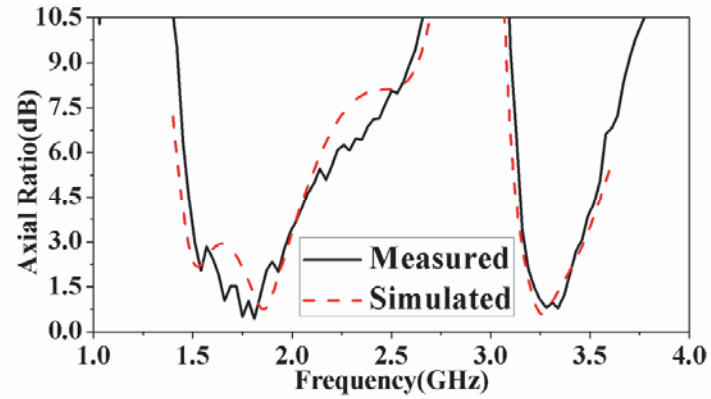

Figure 11. Measured and simulated axial ratio bandwidth of the proposed antenna.

1.8 GHz the antenna radiates right-hand circularly polarized wave, and it shows cross polarization level of approximately $\geq$ 18 dB in the direction of maximum radiation ($+z$) as shown in Figure 14(a). At 3.3 GHz, antenna radiates left-hand circularly polarized wave, and it shows cross polarization level of approximately $\geq$ 20 dB in the direction of maximum radiation ($+z$) as shown in Figure 14(b).

For comparison, previous works are listed in Table 1. The proposed antenna is presented with useful CP, dual-band and dual-polarization related to the works.

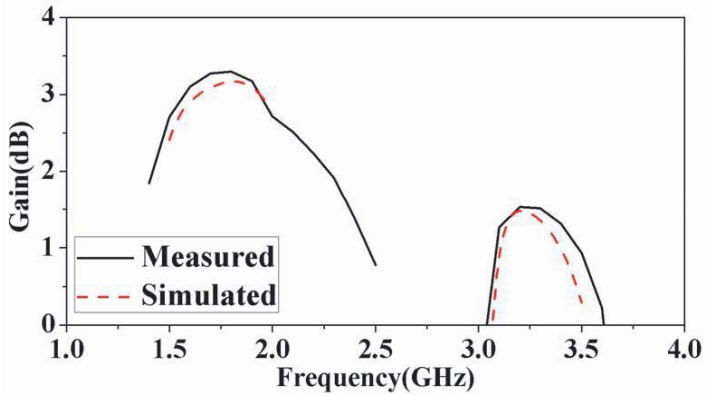

Figure 12. Measured and simulated antenna gains with respect to frequency.

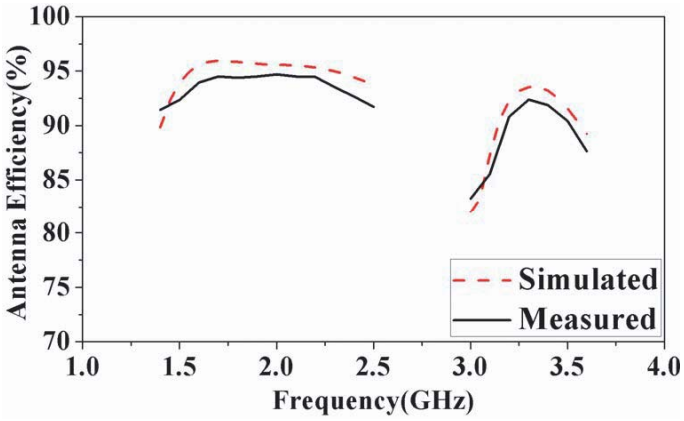

Figure 13. Measured and simulated antenna efficiency with respect to frequency.

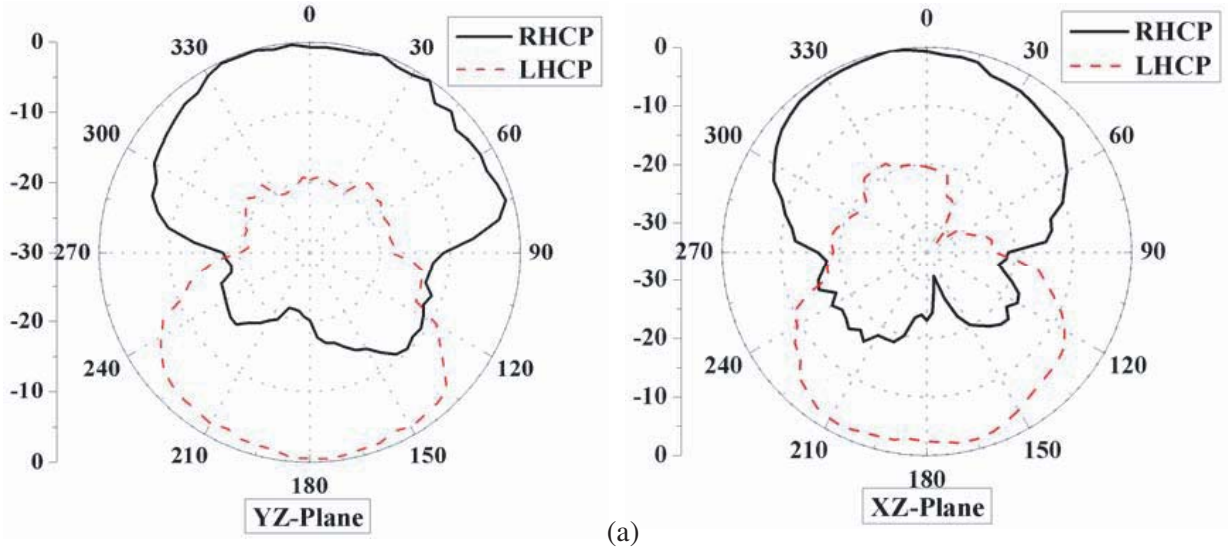

(a)

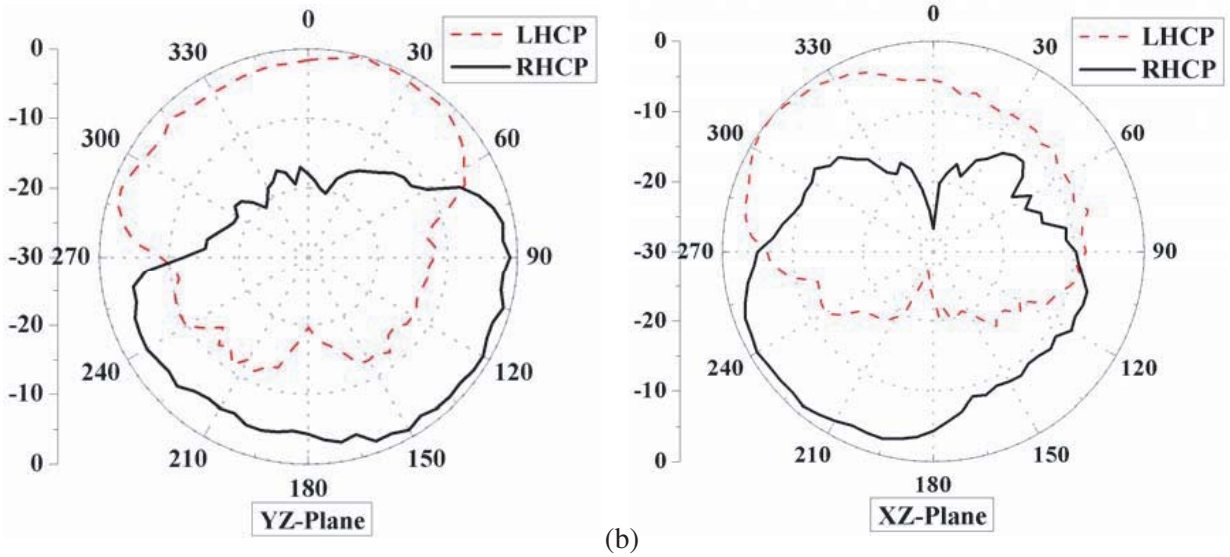

(b)

Figure 14. Measured radiation patterns at (a) 1.8 GHz and (b) 3.3 GHz in both planes (YZ-plane and XZ-plane) of the proposed antenna.

Table 1. Comparison.

	Size; mm^2	Freq.; GHz	Polarization	S_{11} BW%	AR BW%
Ref. [7]	60×50	2.9	RHCP	63.97	48.28
Ref. [8]	70×70	1.54/1.98	LHCP	17/21	9/11
Ref. [9]	70×70	1.6/2.2	DUAL CP	8.7/23	8.4/19.24
Ref. [11]	63×75	2.5/3.5	DUAL CP	71.63	27.45/7.1
Ref. [13]	70×70	1.7/2.55	DUAL CP	106.9	32.35/5.6
Proposed	63.5×55	1.75/3.3	DUAL CP	26.04/18.93	22.22/10.53

7. CONCLUSION

A novel compact dual-band dual-sense circularly polarized CPW-fed slot antenna has been designed. By introducing an F-shaped signal line, parasitic elements and asymmetric slot size, dual-band and dual-sense circular polarization was achieved. The measured impedance and axial ratio bandwidths are 26.04%, 22.22% for the lower band and 18.93%, 10.53% for the upper band, respectively. The proposed antenna provides good CP radiation characteristics with RHCP and LHCP for the lower and upper bands in the $+z$ direction simultaneously. The antenna is expected to be useful in the areas of radar, wireless communication, and navigational systems.

REFERENCES

1. Wang, C.-J. and C.-H. Chen, "CPW-fed stair-shaped slot antennas with circular polarization," *IEEE Trans. Antennas Propag.*, Vol. 57, No. 8, 2483–2486, Aug. 2009.
2. Sze, J.-Y., C.-I. G. Hsu, Z.-W. Chen, and C.-C. Chang, "Broadband CPW-fed circularly polarized square slot antenna with lightening-shaped feedline and inverted-L grounded strips," *IEEE Trans. Antennas Propag.*, Vol. 58, No. 3, 973–977, Mar. 2010.

3. Deng, C., J. B. Chen, Q. X. Ke, C. J. Rong, W. F. Chang, and Y. T. King, "A circular CPW-fed slot antenna for broadband circularly polarized radiation," *Microw. Opt. Technol. Lett.*, Vol. 49, No. 11, 2728–2733, Nov. 2007.
4. Liu, Y. W. and P. Hsu, "Broadband circularly polarized square slot antenna fed by co-planar waveguide," *Electron. Lett.*, Vol. 49, No. 16, 976–977, Aug. 2013.
5. Zhou, S.-W., P.-H. Li, Y. Wang, W.-H. Feng, and Z.-Q. Liu, "A CPW-fed broadband circularly polarized regular-hexagonal slot antenna with L-shape monopole," *IEEE Antennas Wireless Propag. Lett.*, Vol. 10, 1182–1185, 2011.
6. Felegari, N., J. Nourinia, C. Ghobadi, and J. Pourahmadazar, "Broadband CPW-fed circularly polarized square slot antenna with three inverted-L-shape grounded strips," *IEEE Antennas Wireless Propag. Lett.*, Vol. 10, 274–277, 2011.
7. Saini, R. K. and S. Dwari, "CPW-fed broadband circularly polarized rectangular slot antenna with L-shaped feed line and parasitic elements," *Microwave and Optical Technology Letters*, Vol. 57, No. 8, Aug. 2015.
8. Chen, C.-H. and E. K. N. Yung, "Dual-band circularly-polarized CPW-fed slot antenna with a small frequency ratio and wide bandwidths," *IEEE Trans. Antennas Propag.*, Vol. 59, No. 4, 1379–1384, Apr. 2011.
9. Chen, C. and E. K. N. Yung, "Dual-band dual-sense circularly-polarized CPW-fed slot antenna with two spiral slots loaded," *IEEE Trans. Antennas Propag.*, Vol. 57, No. 6, 1829–1833, Jun. 2009.
10. Bao, X. L. and M. J. Ammann, "Dual-frequency dual-sense circularly polarized slot antenna fed by microstrip line," *IEEE Trans. Antennas Propag.*, Vol. 56, No. 3, 645–649, Mar. 2008.
11. Saini, R. K., S. Dwari, and M. K. Mandal, "Dual-band dual-sense circularly polarized monopole antenna," *IEEE Antennas and Wave Propagation Letters*, Vol. 16, Jul. 2017.
12. Saini, R. K. and S. Dwari, "Dual-band dual-sense circularly polarized slot antenna," *International Conference on Electromagnetics in Advanced Applications*, 472–475, Sept. 2017.
13. Chen, Y.-Y., Y.-C. Jiao, G. Zhao, F. Zhang, Z.-L. Liao, and Y. Tian, "Dual-band dual-sense circularly polarized slot antenna with a C-shaped grounded strip," *IEEE Antennas Wireless Propag. Lett.*, Vol. 10, 915–918, 2011.
14. Lai, X.-Z., Z.-M. Xie, and X.-L. Cen, "Design of dual circularly polarized antenna with high isolation for RFID application," *Progress In Electromagnetics Research*, Vol. 139, 25–39, 2013.
15. Saini, R. K. and S. Dwari, "A broadband dual circularly polarized square slot antenna," *IEEE Trans. Antennas Propag.*, Vol. 64, No. 1, Jan. 2016.
16. Saini, R. K. and S. Dwari, "Dual-band dual-sense circularly polarized square slot antenna with changeable polarization," *Microwave and Optical Technology Letters*, Vol. 59, No. 4, Apr. 2017.